Advances in Computer and Communications, 2022, 3(1), 16-22
https://www.hillpublisher.com/journals/acc/
ISSN Online: 2767-2875

Specific Radiation Source Algorithm Based on Modulated Broadband Converter

Jiarui Hao, Zhi Li*

College of Electronics and Information Engineering, Sichuan University, Chengdu, Sichuan, China.

How to cite this paper: Jiarui Hao, Zhi Li. (2022) Specific Radiation Source Algorithm Based on Modulated Broadband Converter. *Advances in Computer and Communication*, 3(1), 16-22.
DOI: 10.26855/acc.2022.06.001

Received: April 15, 2022
Accepted: May 13, 2022
Published: June 27, 2022

***Corresponding author:** Zhi Li, College of Electronics and Information Engineering, Sichuan University, Chengdu, Sichuan, China.
Email: lizhi@scu.edu.cn

Abstract

The nonlinear characteristics of the power amplifier of the radiation source are used as the basis for the classification and identification of the radiation source. The algorithm is divided into the following steps. Firstly, the multi-channel modulation broadband converter (MWC) is used to preprocess the signal, and the compression and sampling of the signal are completed in parallel to obtain two-dimensional compressed sampling data. Then the gray-scale co-occurrence matrix is calculated for this data, and the corresponding features are extracted, and the identification and classification of radiation sources are carried out according to this feature. In order to illustrate the reliability of performance, the algorithm is compared with VMD_SF and MWC_IC algorithms with better identification performance. The results show that the proposed method is obviously better than the comparison algorithm. In addition, because the classification task of radiation sources is completed in the compressed domain, the proposed algorithm's sampling frequency and calculation amount are much lower than the VMD_SF algorithm.

Keywords

Specific radiation source identification, modulated wideband demodulator, non-reconstruction

1. Introduction

In the Specific Emitter Identification (SEI,), we rely on the individual differences between different radiation source transmitter devices to achieve classification identification, this difference is called the radiation source radio frequency fingerprint (RFF). In addition, not all individual differences can be used as fingerprint features, and stability, universality, measurability, and independence are necessary conditions for fingerprint features [1]. By identifying different RFFs, distinguishing between enemy and friendly electronic equipment, and conducting reconnaissance and monitoring of enemy equipment, it provides strong information support for military confrontation. Therefore, research on SEI has important research significance and application value. Compression learning refers to learning directly in the compression domain. Reference [2] pointed out that if the projection matrix can save the inner product (interval) between training samples with a high probability, then it is suitable for compression learning. If the projection matrix satisfies the Johnson-Lindenstrauss characteristic, then this matrix satisfies the distance fidelity property and the constrained isometric property. Therefore, it is possible for us to directly use the compressed sampling matrix of MWC for classification learning, which greatly saves the computational cost of reconstructing signals in traditional compressed sensing and machine learning, and has considerable application prospects.

2. System Model and MWC

2.1 System Model

In the communication system, we can determine the number of radiation sources in the system through the radiation source enumeration algorithm. Considering a single-hop communication model, the nonlinear system of the power amplifier can be described by the Taylor series model, as shown in the following formula:

$$S^{[n]}(x_n) = \sum_{l=1}^{ls} a_l{}^{[n]}(x_n)^l \quad ,n = 1,2,\dots,n \ \# \ (1)$$

in the above formula

$$x_n = s_n e^{j2\pi f tT} \ \# \ (2)$$

s_n is the baseband modulated signal of the nth radiation source, and x_n is the input signal of its power amplifier, which has been modulated to the carrier with frequency f. $a_l{}^{[n]}$ is the coefficient of the Taylor series model of the power amplifier, which has a total of ls order, and $S^{[n]}(x_n)$ is the signal sent by the transmitter after being affected by nonlinearity. We can see that the different Taylor model coefficients add a unique unintentional modulation to the signal when the individual radiation sources are different.

Considering the channel fading and noise effects in the communication system, the signal r_n finally received by the receiver R can be expressed as

$$r_n = \varphi^{[n]}(x_n) + w_n \quad n = 1,2,\dots,n \ \# \ (3)$$

Where $\varphi^{[n]}$ is the signal fading coefficient between the nth individual radiation source and the receiver, and w_n is the additive white Gaussian noise. If Equation (1) is brought into Equation (3), then$r_n$can be expressed as

$$r_n = \varphi^{[n]} \sum_{l=1}^{ls} a_l{}^{[n]}(x_n)^l + w_n \quad n = 1,2,\dots,n \ \# \ (4)$$

2.2 MWC system

The MWC system is suitable for a wideband signal with a sparse multi-subband model. It is assumed that x(t) is a continuous substantial time signal, the highest frequency in its spectrum is $f_{Nyquist}/2$, and the frequency components higher than this value in the signal are 0. If the signal has only N sub-bands with a width not exceeding BHz in the frequency band, these sub-bands do not intersect with each other, and can be distributed in any position of the frequency spectrum, then the signal is a sparse multi-band signal. Figure 1 is a sparse multi-band spectrogram with the number of frequency bands N=4.

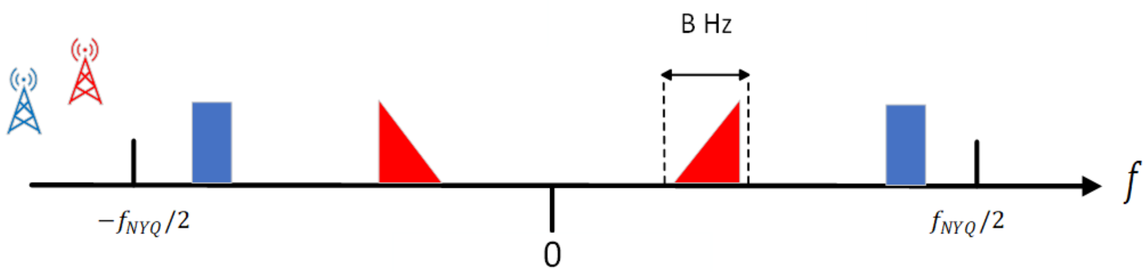

Figure 1. Spectrogram of multi-band sparse signal.

The system is shown in Figure 2. The MWC system as a whole consists of m sampling channels, low-pass filters, and low-speed samplers. The original signal x(t) enters m channels at the same time, and in each channel is mixed with a sequence of pseudorandom symbols $p_{(i)}(t)$ of period $T_{(p)}$. The period of $p_{(i)}(t)$ is $T_{(p)}$, the frequency is $f_{(p)}$ and there are M sequence symbols with amplitude [+1,-1] in one period.

After mixing, the spectrum of the original signal is uniformly moved to each subband, and the signal enters a low-pass filter with a cutoff frequency of $f_s/2$ for filtering. As long as the sampling frequency of the sampler is greater than f_s, the collected data can contain the All information.

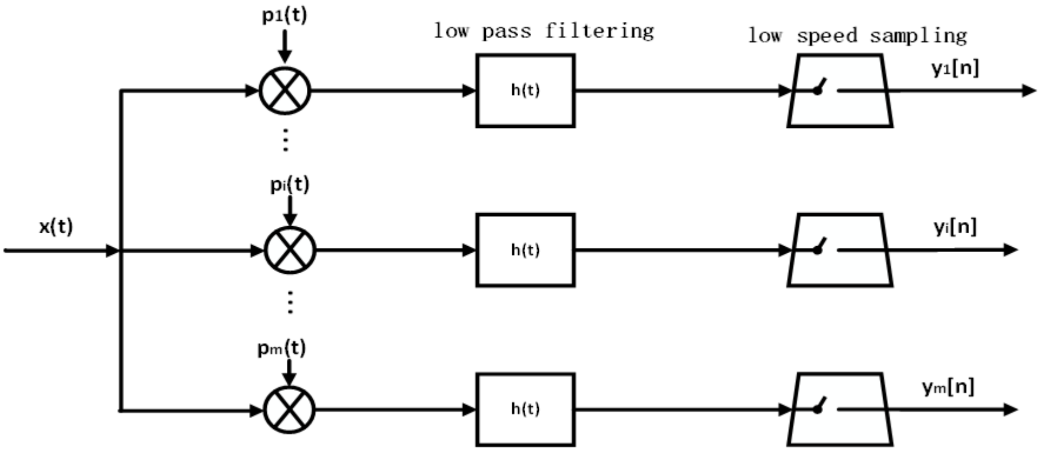

Figure 2. MWC system.

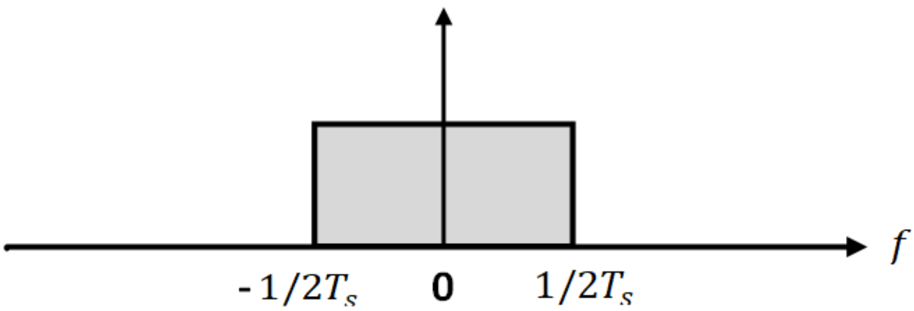

Figure 3. Frequency response of filter h(t).

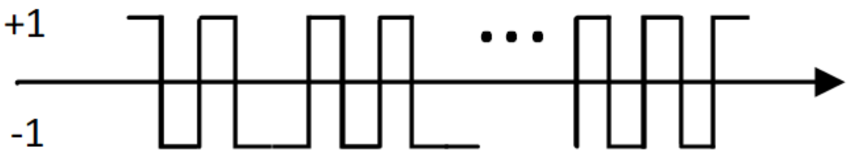

Figure 4. Random mixing sequence.

3. Radiation source identification algorithm based on modulated broadband converter

In the single-hop scenario, the carrier frequency of the signal is high, the amount of processing data is large, and the features are blurred. The MWC is used to sample the compressed sampling data (CSD) of the signal at a low speed. In the case of non-reconstruction, frequency domain transformation and grayscale map mapping are performed on CSD and its grayscale co-occurrence matrix is calculated.

The gray-level co-occurrence matrix usually includes 14 features such as entropy, energy, moment of inertia, local stationary, correlation, contrast, etc., but only four of these texture features are irrelevant, and the second-order moment ASM, entropy ENT, correlation are calculated separately. COR, contrast CON. Each feature is calculated as a matrix of the same size as the original grayscale image, and the first 2 larger values in each feature matrix are selected respectively, and a total of 8 eigenvalues form a eigenvector.

The ASM reflects whether the grayscale is uniform and the texture thickness.

$$ASM = \sum_i \sum_j p(i,j)^2 \# (5)$$

$p(i,j)$ is the value corresponding to row i and column j in GLCM. In addition, ENT reflects the randomness of the texture.

$$ENT = -\sum_i \sum_j p(i,j) logP(i,j) \# (6)$$

COR is the embodiment of the local grayscale correlation of the image

$$COR = (\sum_i \sum_j ij * p(i,j) - \mu_x \mu_y)/\sigma_1^2 \sigma_2^2 \# (7)$$

in the above formula

$$\mu_x = \sum_i i \sum_j p(i,j) \# (8)$$

$$\sigma_1^2 = \sum_i (i-\mu_x)^2 \sum_j p(i,j) \quad \# (9)$$

CON reflects the clarity of the image

$$CON = \sum_i \sum_j p(i,j)^2 \, (i-j)^2 \#(10)$$

For the convenience of description, the algorithm based on MWC and gray level co-occurrence matrix texture features is abbreviated as MWC_TF algorithm. The specific process is shown in the following table.

Table 1. MWC_TF algorithm

MWC_TF algorithm
Training phase: the number of radiation source classes is P, and the number of signal samples for each class is N
1. The original signal is compressed and collected by MWC, and the sampled data matrix A is obtained;
2. Perform a two-dimensional Fourier transform on the matrix A, round it down, and map it into a two-dimensional grayscale matrix B, and calculate the grayscale co-occurrence matrix of the B matrix;
3. Calculate the ASM, ENT, COR, and CON of the gray-level co-occurrence matrix according to the formula (5)-formula (10), and take the first two larger values of each feature matrix to form the feature vector ψ_i;
4. The training sample l_i={ψ_i,ω_i} is composed of the ψ_i obtained in step 3 and the sample labelω_i, and the above steps are repeated to obtain the training sample set, and train the random forest classifier;
Training phase: the number of radiation source classes is P, and the number of signal samples for each class is N
5. Obtain the feature vector ψ_j as in steps 1-3
6. Use the random forest classifier to determine the category of ψ_j

4. Numerical simulation experiment

In this section, the performance difference between the algorithm proposed in this chapter and the comparison algorithm is evaluated through comparative experiments. The comparison algorithm is two algorithms with good recognition performance in the single-hop scenario, namely the VMD_SF algorithm proposed in the literature [3] and the proposed algorithm in the literature [4]. The MWC_IC algorithm. TakingP_c as the performance indicator, it is defined as follows:

$$P_c = \frac{1}{N} \sum_{i=1}^{N} p_{(i)} \quad \# (12)$$

$p_{(i)}$ represents the probability of successfully classifying the i-th radiation source, and N represents the number of radiation sources present in the scene. The baseband signal modulation mode of the transmitter is 16QAM, the signal sampling frequency is $8GHz$, the carrier frequency is $2GHz$, and the length of each signal sample is 20000. After the original signal is compressed and sampled by MWC, the sample length is 100, the compression ratio is 200:1, and the f_{nyq} of the sparse bandwidth signal is set to $10GHz$, fp=fs=50MHz, it can be found that MWC will originally need to sample the signal at a speed of up to 10GHz, After spectrum shifting, the CSD matrix containing spectrum information can be obtained with only 50MHz low-speed sampling, which greatly reduces the sampling cost. After the multi-channel sampling of MWC, a 40 × 100 two-dimensional matrix is finally obtained. The number of training sequences and test sequences for each class is 200 and 100, respectively. A third-order Taylor series is used to model the nonlinear distortion of the PA. The third-order Taylor coefficients of the PA are set as $a1$ = (1,0.5,0.3), $a2$=(1,0.08,0.6), $a3$ = (1 ,0.01,0.4) , $a4$ = (1,0.01,0.1).

Next is a specific simulation experiment, and the recognition performance is evaluated for the cases of N=2, 3, and 4 in the communication system under the Gaussian channel (AWGN) channel.

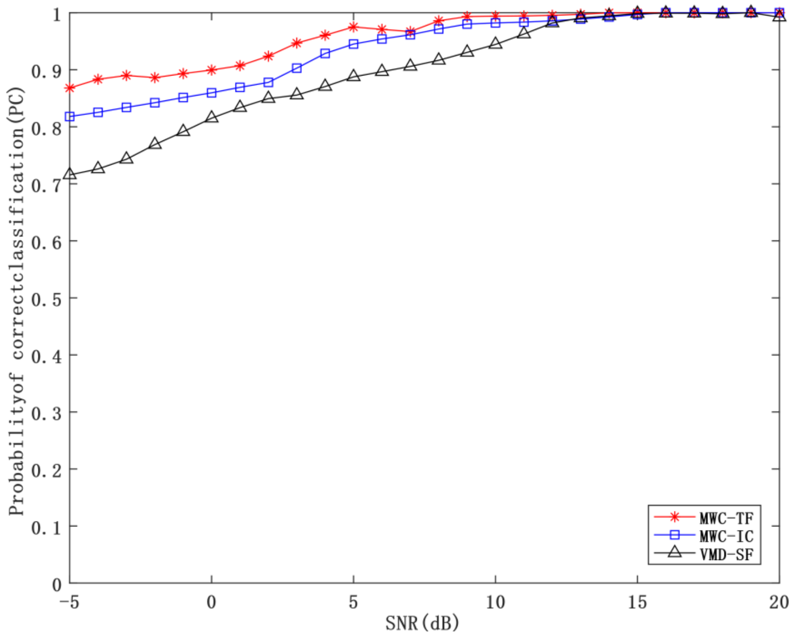

Figure 5. Comparison of recognition performance when N=2.

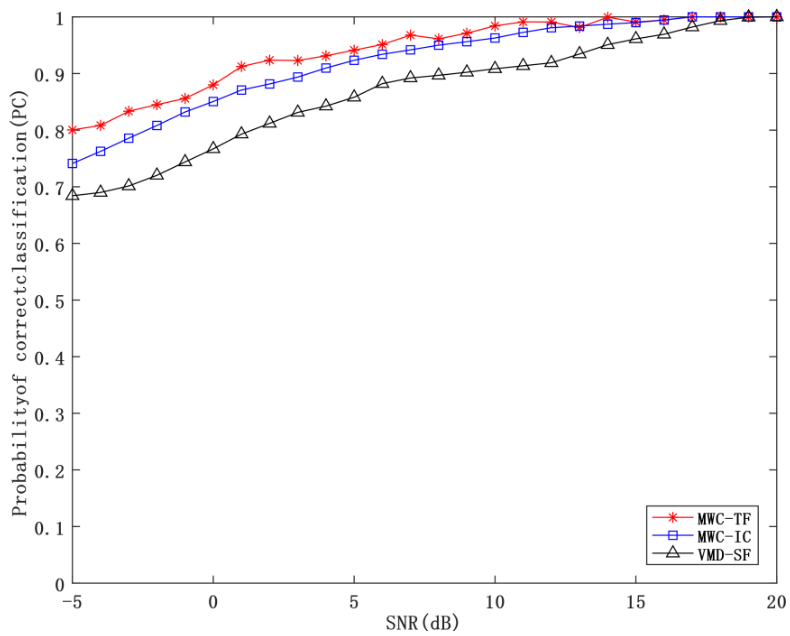

Figure 6. Comparison of recognition performance when N=3.

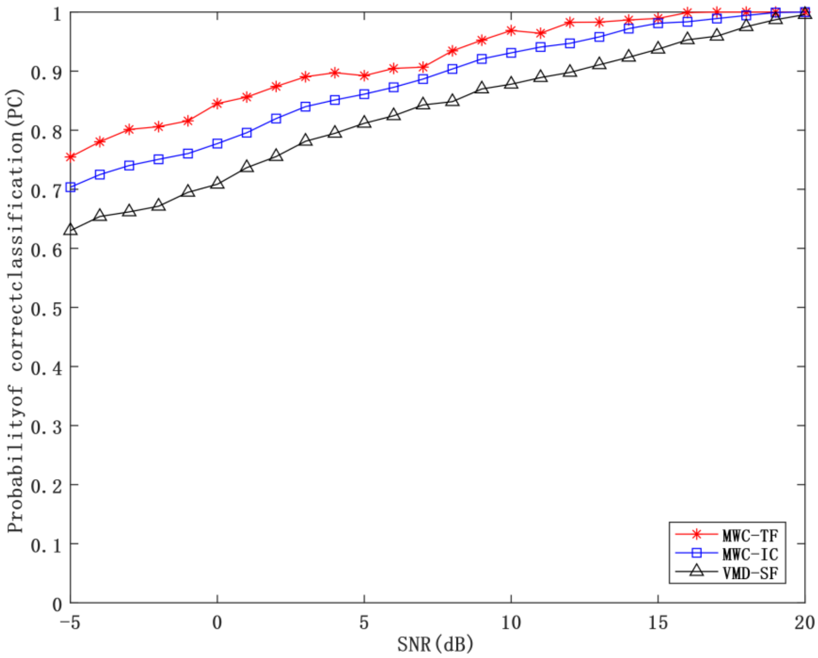

Figure 7. Comparison of recognition performance when N=4.

Because in the single-hop scenario, the signal is directly captured by the signal receiver after the radiation source transmitter is sent out, and there is no repeater in the middle, and the signal only contains the inherent nonlinear fingerprint information of the transmitter. Figures 5-7 compares the MWC_TF algorithm with the MWC_IC and VMD_SF algorithms when the individual types of radiation sources are 2, 3, and 4 in the AWGN channel. It can be seen from the recognition rate curve that the recognition rates of the three algorithms generally increase with the improvement of the signal-to-noise ratio, and the recognition effect of the MWC_TF algorithm proposed in this chapter is better than that of the comparative methods. As can be seen from Figure 5, when N=2, at -5dB signal-to-noise ratio, MWC_TF has a recognition rate of more than 85%. When N=3, N=4, it can be seen that the same MWC_TF algorithm has an advantage in recognition rate compared with the MWC_IC and VMD_SF algorithms under low signal-to-noise ratio.

5. Conclusion

This chapter studies SEI in the single-hop scenario. Aiming at the problems of high carrier frequency band, large signal bandwidth, and large processing data in traditional SEI identification, the MWC system is used to complete signal capture, frequency mixing, filtering, sampling, and obtain compressed sampling data of the signal. After a series of preprocessing, and then the corresponding multiple gray-level co-occurrence matrix features are extracted to complete the classification and identification. Compared with the traditional algorithm, the method proposed in this chapter directly learns the classifier in the compressed domain, and completes the classification and identification of the signal under the condition of non-reconstruction of the signal, which saves a lot of system resources.

The recognition rate of this algorithm is obviously higher than that of MWC-IC algorithm and VMD-SF algorithm under low signal-to-noise ratio, which has obvious advantages. However, due to the direct classification learning from compressed sampled data, the feature preservation of samples and the preservation of distances between samples in low-dimensional space are extremely dependent on the Johnson-Lindenstrauss property of the compressed observation matrix. Therefore, it can be seen that the recognition rate of this algorithm has slight fluctuations in the recognition effect under high signal-to-noise ratio.

Random forest is a classification machine with good performance and strong robustness to noise. In this chapter, random forest algorithm is used to complete the final sample classification work. Simulation experiments show that the overall recognition rate of this algorithm is higher than that of the two contrasting algorithms, especially at low signal-to-noise ratios. The operation cost is greatly reduced, the recognition efficiency is accelerated, and it has certain reference significance for the actual SEI work.

References

[1] Xu Dan. (2008). Research on the mechanism and identification method of radiation source fingerprints [D]. Changsha: National University of Defense Technology, 2008.

[2] Yonina C. Eldar and Gitta Kutyniok. (2018). Compressed Sensing: Theory and Applications [M]. Machinery Industry Press, 2018: 343.

[3] U. Satija, N. Trivedi, G. Biswal, and B. Ramkumar. (2019). "Specific emitter identification Based on Variational Mode Decomposition and Spectral Features in Single Hop and Relaying Scenarios," IEEE Trans. Inf. Forensics Security, vol.14, no.3, pp. 581-591, March 2019.

[4] Xie Jianlan. Research on key feature extraction and identification of individual radiation sources based on modulated broadband converters [D]. Sichuan University.